Published in final edited form as:
J Vis. 2012 ; 12(3): 8. doi:10.1167/12.3.8.

Deconstructing continuous flash suppression

Eunice Yang and **Randolph Blake**
Vanderbilt Vision Research Center, Vanderbilt University, Nashville, TN, USA, Department of Psychology, Vanderbilt University, Nashville, TN, USA, & Department of Brain and Cognitive Sciences, Seoul National University, Seoul, South Korea

Abstract

In this paper, we asked to what extent the depth of interocular suppression engendered by continuous flash suppression (CFS) varies depending on spatiotemporal properties of the suppressed stimulus and CFS suppressor. An answer to this question could have implications for interpreting the results in which CFS influences the processing of different categories of stimuli to different extents. In a series of experiments, we measured the selectivity and depth of suppression (i.e., elevation in contrast detection thresholds) as a function of the visual features of the stimulus being suppressed and the stimulus evoking suppression, namely, the popular “Mondrian” CFS stimulus (N. Tsuchiya & C. Koch, 2005). First, we found that CFS differentially suppresses the spatial components of the suppressed stimulus: Observers' sensitivity for stimuli of relatively low spatial frequency or cardinally oriented features was more strongly impaired in comparison to high spatial frequency or obliquely oriented stimuli. Second, we discovered that this feature-selective bias primarily arises from the spatiotemporal structure of the CFS stimulus, particularly within information residing in the low spatial frequency range and within the smooth rather than abrupt luminance changes over time. These results imply that this CFS stimulus operates by selectively attenuating certain classes of low-level signals while leaving others to be potentially encoded during suppression. These findings underscore the importance of considering the contribution of low-level features in stimulus-driven effects that are reported under CFS.

Keywords

continuous flash suppression; binocular rivalry; interocular suppression

Introduction

Continuous flash suppression (CFS) refers to a potent form of binocular rivalry wherein a visual stimulus presented to one eye is suppressed from awareness as a result of a rapidly changing sequence of high-contrast, contour-rich patterns viewed by the other eye (Tsuchiya & Koch, 2005). The stimulus display first utilized to induce CFS consisted of a montage of different sized rectangles whose luminance and locations varied randomly over time, with each montage resembling a Mondrian pattern. Tsuchiya and Koch (2005), the inventors of this display, did not explain why this particular stimulus design was chosen, but it is the most popular version of CFS display currently in use (Hesselmann & Malach, 2011; Jiang & He, 2006; Kanai, Tsuchiya, & Verstraten, 2006; Kaunitz et al., 2011; Stein & Sterzer, 2011; see Figure S1 and Table S1 for examples of frequently used CFS stimuli). Suppression

Corresponding authors: Eunice Yang and Randolph Blake. eunice.yang@vanderbilt.edurandolphblake@ gmail.com. Department of Psychology, Vanderbilt University, PMB 407817, 2301 Vanderbilt Place, Nashville, TN 37240-7817, USA..

Commercial relationships: none.

generated by this CFS stimulus is so potent that a stimulus viewed by the other eye may remain undetectable for extended periods of time ranging up to a minute or more (Tsuchiya & Koch, 2005; Tsuchiya, Koch, Gilroy, & Blake, 2006). Because of its potency, CFS was quickly picked up as a potentially effective tool for investigating stimulus processing outside of awareness.

The emerging picture from studies using CFS is that visual processing of certain categories of stimuli can occur even when those stimuli are rendered perceptually invisible. Specifically, several studies suggest that the affective and semantic content of a stimulus may be encoded despite suppression from awareness of that stimulus by CFS (review by Lin & He, 2009). Furthermore, some studies report that processing of certain object categories like faces (Jiang, Costello, & He, 2007; Jiang & He, 2006; Sterzer, Jalken, & Rees, 2009, but Stein, Hebart, & Sterzer, 2011; Stein & Sterzer, 2011) and tools (Almeida, Mahon, Nakayama, & Caramazza, 2008; Fang & He, 2005, but Kaunitz et al., 2011) may remain effective even though those objects are rendered invisible by CFS. Before drawing firm conclusions from these tantalizing results, however, it would be useful to understand the extent to which CFS impacts feature components represented in early stages of processing, which provide input to higher stages where those object categories are explicitly represented. It is known already that CFS interferes with encoding of several fundamental visual attributes registered in early vision, including orientation (Kanai et al., 2006), spatial phase (Tsuchiya & Koch, 2005), motion (Maruya, Watanabe, & Watanabe, 2008), and contrast (Shin, Stolte, & Chong, 2009; Tsuchiya et al., 2006; Yang, Hong, & Blake, 2010). Our study extends this analysis by investigating the extent to which the effectiveness of CFS depends on the spatiotemporal properties of the stimulus evoking suppression and of the stimulus being suppressed. To explore this spatiotemporal feature space, we selected the CFS stimulus that has been most frequently used in earlier work, i.e., the CFS display invented by Tsuchiya and Koch (2005). We employed a test probe technique that has been widely used for decades to examine the selectivity and depth of interocular suppression associated with binocular rivalry (Alais, Cass, O'Shea, & Blake, 2010; Blake, Yu, Lokey, & Norman, 1998; Nguyen, Freeman, & Wenderoth, 2001; Wales & Fox, 1970).

Experiments 1 and 2: Spatial properties of the suppressed stimulus

These experiments systematically measured the effects of CFS on the ability of observers to detect targets that varied over a wide range of spatial frequencies (Experiment 1) and orientations (Experiment 2). A forced-choice, staircase technique was used to estimate contrast thresholds for detecting probes presented to the target eye when that eye was suppressed by a CFS display (CFS condition) and when it was not suppressed (baseline condition). If CFS does indeed exert differential effects on processing of stimuli with different spatial features, detection thresholds in the CFS condition should vary depending on the spatial features of the suppressed stimulus. However, if CFS operates uniformly on all spatial features, elevations in detection thresholds should be comparable in magnitude relative to baseline measures. The CFS display used throughout this study consisted of Mondrian patterns very similar to those used in many other published CFS studies (e.g., Hong & Blake, 2009; Jiang & He, 2006; Tsuchiya & Koch, 2005).

General methods

Participants—Six observers including one of the authors participated in each experiment. Nineteen different observers participated across the experiments with the exception of a few (5) who participated in 2 or 3 experiments. Observers were recruited from the Vanderbilt University Psychology Department and from the local Nashville area. All had normal or corrected-to-normal acuity and good stereopsis. Participants (except the author) were naive to the purpose of the study and provided written consent prior to participation.

Apparatus—Stimuli were presented on the left and right halves of a gamma-corrected CRT monitor (21″ Sony Multiscan; 1024 × 768 resolution; 100-Hz refresh rate) and were viewed at a distance of 92 cm in a darkened room. Stimuli were generated and displayed on a G4 Power Macintosh computer running MATLAB supplemented by the Psychophysics toolbox (Brainard, 1997; Pelli, 1997). All experiments employed 10-bit luminance resolution using a "bit stealing" technique (Tyler, 1997). Stimuli were viewed through a mirror stereoscope with mounted chin and head rests, which presented the stimulus in the right half of the display exclusively to the right eye and the stimulus in the left half of the display exclusively to the left eye. Binocular fusion contours surrounding the stimuli and fixation dots were present at all times to promote stable binocular eye alignment. Stimuli were always presented against a uniform gray background at mean luminance (15 cd/m^2).

Methods

Stimuli—The target (to-be-suppressed) stimulus in Experiment 1 was a circular Gabor patch (sinusoidal grating enveloped by a Gaussian) for one group of participants and a face image for a different group of participants. The Gabor patch (1° radius) was presented at one of six spatial frequencies: 0.5, 1, 2, 4, 8, or 12 cpd (Figure 1). It was oriented either 10° clockwise or counterclockwise of vertical and the orientation and phase (180° reversal) were randomly chosen for each trial. The Gabor patch was embedded in weak, 1D broadband Gaussian noise (2° × 2°, 10% root mean square or RMS contrast). The face stimuli were two front-facing images (one male) with neutral expressions selected from the Karolinska Database of Emotional Faces (Lundqvist & Litton, 1998). Face stimuli were cropped (2° × 1.5°) to remove features outside of the face and were then scaled to gray and normalized in contrast (50% RMS contrast) and mean luminance. See methods in Experiment 3 for description of the spatial frequency band-pass filtering procedure. The center frequencies for the low and high band-pass filters were 0.75 cpd and 6 cpd, respectively, with an octave wide bandwidth (Figure 1). The spatial frequency filtered face stimulus was embedded in weak, 1D broadband Gaussian noise (4° × 4°, 10% RMS contrast). The center–center distance between the face stimulus and background noise (fixation) was approximately 1°, and across trials, the face stimulus was randomly positioned in one of the two vertical halves of the background noise. The contrast of the target stimulus (Gabor patch or face image) varied across trials and was determined by an adaptive staircase procedure.

The target stimulus in Experiment 2 was an achromatic noise pattern (4° × 4°; 10% RMS contrast) band-pass filtered in the orientation domain (20° bandwidth), with orientation frequencies centered either at 0°, 45°, 90°, or 315° (where 0° denotes vertical; Figure 1). The noise pattern was also spatial frequency band-pass filtered (<19 cpd) to minimize artifacts. Filtering was performed in the Fourier domain using a 2D Finite Impulse Response filter and smoothed to reduce aliasing. The probe was a brief contrast increment (3° × 2° aperture with smoothed edges) that occurred in either the top or the bottom part of the noise pattern, symmetrically positioned with respect to a central fixation mark.

The CFS display consisted of a dynamic series of randomly generated achromatic Mondrian patterned images made of rectangles drawn in variable size (0.2° – 1.2° in length), luminance, and location within a 2° (Experiment 1 with Gabor patch as target stimulus) or 4° (Experiment 1 with face as target stimulus and Experiment 2) square aperture of uniform luminance (15 cd/m^2). The Mondrian images changed every 100 ms throughout a trial. The CFS display was normalized in mean luminance (15 cd/m^2) and RMS contrast, which was determined individually for each observer prior to the experiment.

Procedure for Experiment 1—On each trial, a target stimulus (a Gabor patch or a face image superimposed on noise) of a given spatial frequency was presented to one eye; the

other eye viewed either a dynamic CFS display (CFS condition, as shown in the top part of Figure 1) or a uniform field at mean luminance (baseline condition, not shown). The contrast of the target stimulus gradually ramped to its full magnitude within the noise pattern during the initial 300 ms to avoid abrupt transients. The target stimulus remained at a set contrast determined by a staircase procedure for 1 s. In the remaining 300 ms of a trial, the target stimulus decreased in contrast to reduce subsequent negative afterimages. Once stimuli were removed, observers made their response for a 2-alternative forced-choice (2AFC) orientation or spatial discrimination task, indicating whether the Gabor stimulus was oriented clockwise or counterclockwise of vertical or whether the face image appeared on the left or right side relative to fixation. Observers participated in 2 or 4 sessions: half was devoted to the measurement of contrast detection thresholds when the target stimulus was suppressed with CFS and the other half was devoted to baseline threshold measurements when CFS was absent. Contrast threshold estimates corresponding to 75% accuracy in performance (Watson & Pelli, 1983) were obtained using 2 or 4 randomly interleaved staircases; 4 estimates were obtained for each Gabor spatial frequency condition and 8 estimates were obtained for each band-pass filtered face condition. The conditions were blocked within a session and the order of conditions was randomized and counterbalanced across sessions. Practice trials were performed prior to the first session and the experiment (for each group of participants) took approximately 2 h to complete.

Procedure for Experiment 2—At the beginning of a trial, an orientation band-pass filtered noise stimulus of a given center orientation (0°, 45°, 90°, or 315°) was presented to one eye while the corresponding retinal location of the other eye viewed a dynamic CFS display or a uniform field at mean luminance (baseline), depending on the session. Five-hundred ms after trial onset, the probe (a localized increment in contrast) gradually emerged and remained present for 500 ms. The contrast of the probe was varied over trials according to a staircase procedure. A trial lasted 1 s after which stimuli were immediately replaced by a mask stimulus (high-contrast noise image) to reduce possible negative afterimages. Observers made a 2AFC judgment about the location (above or below fixation) of the probe stimulus. Experiment 2 consisted of 2 sessions, the first in which baseline threshold measurements for probe detection were obtained in the absence of CFS and the second in which contrast thresholds were obtained when the target stimulus was paired dichoptically with the CFS display. Threshold estimates corresponding to 71% correct performance (Levitt, 1971; Tsuchiya et al., 2006) were obtained for each condition using 4 randomly interleaved staircases. Trials for each condition were blocked and the order of blocks was randomized across sessions. Practice trials were performed prior to each session, and the experiment took approximately 1.5 h to complete.

Results

Elevations in contrast threshold produced by CFS were indexed by the log ratio of the mean threshold estimate for a given condition obtained with CFS to the mean baseline estimate for that same condition obtained without CFS. This threshold elevation index serves as our measure of the magnitude of suppression, with higher values indicating stronger suppression.

On the task utilizing a Gabor patch as the test target (Figure 2, left-hand graph), contrast thresholds for discriminating the targets' orientation were elevated relative to baseline for all spatial frequencies, but for all six observers the magnitude of this elevation in threshold was greatest at lower spatial frequencies. A one-way ANOVA on threshold elevation index values revealed that this effect of spatial frequency was highly significant ($F(5,25) = 38.2$, $p < 0.001$). The same outcome was evident in the contrast thresholds measured for the face location task (Figure 2A, inset): Thresholds were significantly higher ($t(5) = 10.2$, $p < 0.001$)

when the spatial frequency content of the band-pass filtered face was only low spatial frequency (mean and standard error: 0.87 ± 0.08 log unit) in comparison to when its content was only high spatial frequency (0.43 ± 0.05 log unit). Incidentally, we elected to perform this face probe experiment to determine whether the differential effect of CFS on spatial frequency so clearly evident when using Gabor patches would generalize to more familiar, complex images. We did not construe the face task as a way to tap into higher level visual processing; indeed, our task simply involved measuring the contrast needed to detect the location of the face probe and did not measure performance in face identification (Alais & Melcher, 2007).

Turning to the results from Experiment 2, we found a significant effect of probe orientation on the threshold elevation index ($F(3,15) = 4.4$, $p = 0.02$; Figure 2B). CFS produced greater elevations in thresholds for vertically oriented probes (0.29 ± 0.04 log unit) compared to threshold elevations produced by either of the oblique conditions (45°: $t(5) = 4.2$, $p = 0.009$; 315°: $t(5) = 2.6$, $p = 0.05$). Similarly, the difference in threshold elevation for horizontally oriented probes (0.34 ± 0.05 log unit) and probes oriented at 315° (0.22 ± 0.07 log unit) was close to significant ($t(5) = 2.2$, $p = 0.08$). No other comparisons reached significance. When averaging the cardinal and oblique conditions separately, it is evident that CFS produced a greater relative threshold elevation for detecting cardinal orientations (0.33 ± 0.03) in comparison to detecting oblique orientations (0.2 ± 0.06, $t(6) = 3.3$, $p = 0.02$). Data from 5 of 6 observers showed a similar pattern of results and the remaining participant showed no difference among these conditions. This finding that cardinal orientations are more strongly suppressed is not the consequence of obliquely oriented stimuli being generally stronger, for its baseline thresholds without CFS were equivalent to baseline thresholds measured for the cardinal orientations. This equivalence of baseline thresholds for the particular noise probes we used is to be expected according to a recent study on the role of spatial frequency and orientation bandwidth on pattern contrast perception (Hansen & Essock, 2006).

Discussion of Experiments 1 and 2

In their original paper introducing CSF, Tsuchiya and Koch (2005) mention a pilot experiment in which they measured how long a Gabor patch viewed by one eye remained suppressed when the other eye viewed a CFS display very much like the one used in our study. They reported that high spatial frequency Gabor patches remained suppressed for shorter durations than did low spatial frequency Gabors, suggesting that their dynamic Mondrian display was producing feature-dependent suppression. The results from our Experiments 1 and 2 (using a probe technique) point to the same conclusion by quantifying the dependence of suppression depth on spatial frequency and, moreover, on orientation. To reiterate, our results reveal that CFS depresses contrast sensitivity more at low spatial frequencies and at cardinal orientations. This dependence of suppression depth on spatial properties was seen for Gabor patches and for face images.

A ready explanation for these results emerges when we consider the Fourier amplitude spectrum of the Mondrian display used to produce CFS. Figure 3 shows the 1D and average 2D Fourier representations of 1000 randomly generated Mondrian patterns of the kind used in our study. This figure characterizes the distribution of stimulus energy among different spatial frequencies and orientations. As shown, the effective spectral power of these Mondrian patterns is strongest at low spatial frequencies and at cardinal orientations. As we found, it is probes with these spatial features (i.e., low spatial frequencies and cardinal orientations) that are most strongly suppressed by this CFS display. It is natural to surmise that the selectivity and depth of suppression are being governed by the strength of the spatial components of the CFS stimulus. If that is true, then changing the spatial profile of the CFS stimulus should alter the pattern of suppression produced by that CFS stimulus. The following experiments directly test this prediction.

Experiment 3: Spatial structure of the CFS stimulus

This experiment asks whether variations in the spatial frequency content of a CFS display impact suppression depth, as gauged by contrast detection thresholds for probes presented to the suppressed eye. To distinguish the effects of different spatial frequencies comprising the CFS display, Mondrian images were passed through a band-pass filter that preserved a given band of frequencies while rejecting frequencies outside this band.

Methods

Stimuli—The target stimulus was an annular sinusoidal grating (radius = 1.4°), the spatial frequency of which was 0.75, 1.5, 3, 6, or 12 cpd. As in Experiment 1, the grating was oriented either 10° clockwise or counterclockwise from vertical, and its orientation and phase were randomly selected across trials. The annulus was embedded in 1D broadband Gaussian noise (4° × 4°, 15% RMS contrast) and its edges were spatially smoothed with a Gaussian filter.

The CFS displays (4° × 4°) were Mondrian images (rectangle length between 0.5° and 1.4°, 100-ms intervals) generated in an identical manner to those used in the previous experiments. In 5 of 6 CFS conditions, the CFS display was spatial frequency band-pass filtered through the following steps. The 2D Fast Fourier Transform (FFT) was used to represent each image in the Fourier domain. A radial band-pass filter (i.e., 2D Finite Impulse Response filter smoothed with a Butterworth filter to minimize artifacts) was applied to each Fourier-transformed image, such that the radial distance from the origin was directly proportional to the desired spatial frequency range. The center frequencies for the band-pass filters were 0.75, 1.5, 3, 6, or 12 cpd (identical to the frequencies of the grating stimuli) with an octave-wide bandwidth. The desired spectral components were also scaled in order to equate spectral density across different band-pass filtered images. The DC component was set to 0 prior to the filtering process and afterward rescaled to mean luminance before the resulting filtered image was inverse Fourier transformed. All band-pass filtered and unfiltered Mondrian images were normalized in mean luminance (15 cd/m^2) and RMS contrast, which was determined individually for each observer prior to the experiment (see Figure S2 for examples of band-pass filtered CFS images).

Procedure—The procedure was similar to Experiment 1. On each trial, a grating stimulus of a given spatial frequency and orientation was presented to one eye while the other eye viewed at the corresponding retinal position a uniform field at mean luminance (baseline) or a dynamic CFS display of a given spatial frequency composition; baseline and CSF testing was performed in different sessions. The probe grating appeared superimposed within a weak noise field, and the probe's contrast was ramped up during the initial 300 ms to avoid abrupt transients. The probe remained at a set contrast predetermined by a staircase procedure for the remaining 300 ms of the trial. A trial lasted 600 ms after which the stimuli were immediately replaced by a mask stimulus (high-contrast noise image). As before, observers performed a 2AFC orientation discrimination task, indicating whether the probe grating was oriented clockwise or counterclockwise relative to vertical.

The experiment was divided into 6 sessions, each performed on separate days. The first session measured baseline contrast thresholds for orientation discrimination when the grating stimulus was presented without CFS. In the remaining sessions, gratings at one of 5 given spatial frequencies (0.75, 1.5, 3, 6, or 12 cpd) were presented in every combination with CFS displays of 6 different band-pass spatial frequency ranges (center frequency at 0.75, 1.5, 3, 6, or 12 cpd), including an unfiltered (i.e., broadband) version. The 30 conditions were separated into 5 sessions such that each grating condition and each CFS condition were presented at least once within a session. Four randomly interleaved staircases

converging at threshold estimates of 75% correct performance (Watson & Pelli, 1983) were executed for each condition within a block of trials, and the order of blocks was randomized across sessions. Practice trials were performed prior to the first and second sessions. Each session lasted approximately 45 min, and the experiment required a total of approximately 5 h to complete.

Results

As before, we calculated threshold elevation indices for each condition, and those indices were entered into a 6 (CFS spatial frequency range) × 5 (grating spatial frequency) repeated measures ANOVA. The main effects of CFS spatial frequency ($F(5,25) = 8.1$, $p < 0.001$) and grating spatial frequency ($F(4,20) = 10$, $p < 0.001$) were significant. Of particular interest, the interaction between the spatial frequency of the CFS and grating stimuli was significant ($F(20,100) = 6.1$, $p < 0.001$).

Figure 4 shows the pattern of threshold elevations for each of the 5 spatial frequency gratings (denoted by different colored bars) as a function of different band-pass filtered CFS displays (center frequency values expressed on the abscissa). The bar graphs in the upper part of the figure show the threshold elevation index for each of the five probe spatial frequencies tested at each of the six conditions of CSF spatial frequency; the plots in the lower part of the graph summarize the magnitude of threshold elevation produced by each of the five different filtered CFS displays normalized to the threshold elevation produced by the unfiltered CFS. Several features of these results stand out. First, the unfiltered CFS display produced higher threshold elevations at lower probe spatial frequencies. A similar pattern of threshold elevations occurred at the two lowest band-pass filtered CFS displays (center frequencies of 0.8 cpd and 1.5 cpd); the interaction between CFS condition (unfiltered vs. 0.8 cpd; unfiltered vs. 1.5 cpd) and grating spatial frequency was not significant (ps > 0.05). As the center frequency of the CFS band-pass filter increased, however, low spatial frequency probes were less and less affected by CFS; the interaction between CFS center frequency and probe spatial frequency reached significance (unfiltered vs. 3 cpd: $F(4,20) = 2.3$, $p = 0.09$; unfiltered vs. 6 cpd: $F(4(20) = 7.3$, $p = 0.001$; unfiltered vs. 12 cpd: $F(4,20) = 11.1$, $p < 0.001$). Moreover, overall threshold elevations were reduced relative to elevations produced by the unfiltered CFS display, especially for the highest band-pass filter condition (12 cpd: $t(5) = 4$, $p = 0.01$).

Discussion

Replicating the findings of Experiment 1, the results from Experiment 3 confirm that information composed of low spatial frequencies is more strongly suppressed than high spatial frequency information by the CFS display. Furthermore, the pattern in threshold elevation observed with unfiltered CFS can be reproduced using CFS displays composed solely of low spatial frequency information; in stark contrast, CFS displays composed of high spatial frequencies only produced comparatively little threshold elevation overall and hardly none for low spatial frequency probes. As pointed out earlier, the spectral energy in this and other commonly used Mondrian patterns resides primarily in the low spatial frequency region of the spectrum (Figure 3). It is worth noting that some studies have created robust CFS using dynamic displays comprising small, dense figures other than Mondrian-like patterns (Adams, Gray, Garner, & Graf, 2010; Bahrami, Lavie, & Rees, 2007; Costello, Jiang, Baartman, McGlennen, & He, 2009; Maruya et al., 2008; Sterzer et al., 2009). Our analysis of several of those displays reveals that they, too, have energy spectra biased toward low spatial frequencies (Figure S1). We believe, therefore, that the fabled potency of CFS to erase a complex, interesting visual image from awareness arises primarily from its low spatial frequency components, with the high spatial frequency components contributing relatively little to the process. In Experiment 3, we did not vary the

orientation content of the CFS displays, so we cannot say for certain whether the orientation-selective suppression seen in Experiment 1 arises from the orientation components of the CFS stimulus itself.

The rectangular components comprising the CFS display we have used still appear to have sharp edges even when those displays contain only high spatial frequencies. The presence of these sharp luminance discontinuities is not surprising of course (e.g., Campbell & Robson, 1968), but as noted above, high-pass filtered CFS displays nonetheless provoke relatively weak suppression, even when their total spectral power matches that of the unfiltered CFS display. Indeed, the small elevations in contrast thresholds produced by high-pass filtered CFS displays (~0.3–0.5 log unit) match rather closely the sensitivity losses typically found with conventional binocular rivalry stimuli (Blake, Tadin, Sobel, Raissian, & Chong, 2006; Nguyen et al., 2001; Wales & Fox, 1970). Evidently, the sharp edges contained in the high-pass CFS are insufficient to empower CFS, and neither are they necessary as evidenced by the strong suppression produced by blurred low-pass filtered CFS displays. Of course, abrupt discontinuities in luminance also occur over time within conventional CFS displays, and this led us to wonder whether depth of suppression also depends on the temporal structure of the CFS display producing that suppression.

Experiment 4: Temporal structure of the CFS stimulus

In virtually all of the previous studies that have used the CFS procedure, the dynamic CFS display has entailed repetitive presentations of different stimuli at the rate of 10 presentations/s (e.g., Bahrami et al., 2007; Kang, Blake, & Woodman, 2011; Stein et al., 2011). This particular dynamic rate was the one endorsed and verified by Tsuchiya et al. (Tsuchiya & Koch, 2005; Tsuchiya et al., 2006). In our final experiment, we have examined the extent to which the temporal structure of the CFS display influences the suppression it exerts on a stimulus presented to the other eye.

As a reminder, the CFS sequence in our experiment consists of briefly presented, grayscale Mondrian patterns that change abruptly and repetitively over time. With the stimulus frame rate employed by us, a cluster of pixels defining each and every rectangle within the Mondrian changes in luminance every 100 ms; as pointed out in the previous paragraph, this time configuration has been used in many studies. One can construe this form of temporal modulation to be a degenerate version of 5-Hz on/off (i.e., square-wave) flicker, and indeed, these sharp changes in luminance over time produce a very broad spectrum of temporal frequency energy whose peak occurs at 5 Hz. What are the relative contributions of low versus high temporal frequencies to the potency of CSF? Our last experiment sought to answer that question.

Methods

Stimuli—For every trial, 10 grayscale Mondrian images (5° × 5°, 0.5°–1.4° rectangle length) were randomly generated to produce a CFS display in which each image repeated for 10 consecutive frames in a 100-frame sequence (1 s). The time series in luminance change for every pixel within a CFS display was Fast Fourier transformed and band-pass filtered in the temporal frequency domain by removing the sinusoidal components either below (high-pass) or above (low-pass) 10 Hz. To account for anisotropies in the temporal amplitude spectrum of the original (unfiltered) time course, the amplitudes of the remaining temporal components were scaled such that spectral densities were equated across different band-pass filtered sequences. The DC component was set to 0 in the beginning of the temporal filtering process and afterward rescaled to mean luminance (15 cd/m^2) before the resulting filtered spectrum was inverse Fourier transformed. The image sequence was then normalized in mean luminance and RMS contrast (Movies S1 and S2).

The target stimulus was a noise patch (5° × 5°; 15% RMS contrast) that was spatial frequency band-pass filtered in the Fourier domain using a 2D Finite Impulse Response filter and smoothed to reduce aliasing. The spatial frequency band of the noise patch was centered at 1.5 cpd or 8 cpd with an octave-wide bandwidth. The probe was a brief contrast increment (1.6° × 4.3° aperture with smoothed edges) that occurred in either the top or bottom part of the noise stimulus, symmetrically positioned with respect to a central fixation mark.

Procedure—A spatial frequency band-pass filtered noise stimulus was presented to one eye while the corresponding retinal position of the other eye viewed a CFS display or uniform field at mean luminance, depending on the session. To allow for the potential accumulation of suppressive effects produced by successive flashes (Tsuchiya et al., 2006), the probe was introduced 500 ms after trial onset and gradually emerged and disappeared for 500 ms (peak at 250 ms) either above or below fixation. The contrast increment was determined by a staircase procedure. A trial lasted 1 s after which the stimuli were replaced by a mask stimulus (high-contrast noise image). Observers performed a 2AFC detection task, indicating the location of the probe relative to fixation.

The experiment consisted of 3 sessions in which contrast thresholds were estimated for detecting low and high spatial frequency band-pass filtered probe stimuli. The first session obtained baseline measurements in which CFS was absent. In the remaining sessions, CFS displays were either low temporal band-pass filtered, high temporal band-pass filtered, or unfiltered. Each temporal CFS condition was paired with each of the 2 spatial frequency filtered probe stimuli, resulting in 6 different conditions. All conditions were counterbalanced and presented in random order in each session. Trials for each condition were blocked, and two staircases were randomly interleaved within each block. Four threshold estimates corresponding to 71% performance were obtained for each condition (Levitt, 1971). Practice trials were performed prior to each session, and the experiment took approximately 2.5–3 h to complete.

Results

Threshold elevation indices were entered into a 3 (CFS temporal filter) × 2 (probe spatial frequency) repeated measures ANOVA (Figure 5). The main effects of probe condition ($F(1,5) = 11.1$, $p = 0.02$) and CFS condition ($F(2,10) = 7.4$, $p = 0.01$) were statistically significant, but the interaction between the two was not. Consistent with previous experiments, CFS again produced nearly 3 times greater threshold elevation for detecting low spatial frequency probes (0.25 ± 0.04) in comparison to high spatial frequency probes (0.09 ± 0.02). A CFS display that consisted of only low temporal components was as effective at suppressing high (0.09 ± 0.02) and low spatial frequency probes (0.27 ± 0.03) as an unfiltered CFS display (high: 0.13 ± 0.03; low: 0.28 ± 0.02; ps > 0.05). However, a CFS display consisting of only high temporal components was not as effective at suppressing either spatial frequency probes (low: 0.19 ± 0.06, $t(5) = 2.2$, $p = 0.08$; high: 0.03 ± 0.02, $t(5) = 2.9$, $p = 0.03$) in comparison to an unfiltered CFS display.

Discussion

An unfiltered CSF sequence comprises repetitive, sharp luminance changes over time, thereby generating energy over a broad spectrum of temporal frequencies that peaks at 5 Hz. A CFS display with the high temporal frequencies removed (low-pass filtered) exhibits no sharp transients but, nonetheless, remains as effective in suppression as an unfiltered CFS display. In contrast, a CFS display that consists of energy only within the high temporal frequency range (high-pass filtered) appears to have rapid, abrupt luminance changes and yet is less effective at producing strong suppression.

In addition, the relative bias in suppression for low spatial frequencies is still observed with both low- and high-pass temporal filtered CFS displays. It is possible that the temporal structure of CFS further increased the imbalance in suppression of the spatial frequency domain beyond that of its spatial properties. This would explain the results from Experiment 3 in which there was residual suppression of low spatial frequencies by high spatial frequency band-pass filtered CFS displays. However, since the natural spatial profile of the CFS stimulus was preserved across all conditions (i.e., energy was concentrated mostly in low spatial frequencies), it is difficult to determine to what extent the temporal components of CFS contributed further to the low spatial frequency bias in suppression in the current experiment. Together, the results of Experiments 3 and 4 suggest that, during the presentation of a CFS display, the sharp transitions in luminance change over space and time contribute relatively little to the robust suppression produced by that CFS display.

General discussion

Our study systematically investigated the depth and selectivity of suppression produced by CFS in terms of the spatial properties of stimuli viewed by the suppressed eye and the spatiotemporal properties of the CFS evoking suppression. Our results reveal that CFS differentially impairs contrast thresholds for detecting a stimulus depending on the spatial properties of that stimulus: Stimuli composed of low spatial frequencies (Experiment 1) or cardinally oriented features (Experiment 2) are more adversely affected by CFS than are stimuli composed of high spatial frequency or obliquely oriented features. These results are not surprising when we take into account the spatiotemporal composition of the CFS used in our experiments, which is biased toward low spatial frequencies and cardinal orientations (Figure 3). The importance of the spatial frequency content of a CFS display is further underscored by our finding that a CFS display only composed of its low spatial frequency components (Experiment 3) produces elevations in contrast threshold comparable to those measured with an unfiltered CFS stimulus; in comparison, a CFS display only composed of its high spatial frequency components weakly elevates thresholds. CFS-dependent suppression is also observed in the temporal domain (Experiment 4) where we find that a CFS display containing only low temporal frequency components retains its effectiveness whereas a filtered CFS display consisting of only its higher temporal components produces weak depth of suppression. Considered together, these results provide clear evidence that the depth of suppression engendered by CFS depends jointly on the spatiotemporal composition of the CFS and the stimulus it is competing with. As an aside, some investigators favor using colored Mondrian patterns (Carmel, Arcaro, Kastner, & Hasson, 2010), but in pilot work in preparation for our study, we found that color added nothing to the depth of suppression produced in our displays (see Supplementary materials for a summary of that experiment and its results).

We see some similarities between characteristics of suppression obtained with CFS and characteristics of suppression associated with more conventional binocular rivalry stimuli. For one thing, our results reveal that a CFS stimulus composed of only low spatial frequency components is a relatively stronger suppressor than one composed only of high spatial frequencies. The same tendency has been described for conventional binocular rivalry stimuli, where the strength of suppression was gauged by the durations of dominance, suppression, and mixtures of those stimuli (e.g., Hollins & Hudnell, 1980; O'Shea, Sims, & Govan, 1997; Y. Yang, Rose, & Blake, 1992, but see Fahle, 1982). For another thing, we find that CFS induces feature-selective suppression, meaning that losses in visual sensitivity during suppression were strongest when the test probe viewed by one eye and the CFS display viewed by the other eye overlapped in spatial frequency. In addition, an earlier study using the probe technique showed that CFS is also chromatic selective (Hong & Blake, 2009). Conventional binocular rivalry, too, appears to be feature selective, as evidenced by

changes in suppression depth for test probes varying in spatial frequency (Stuit, Cass, Paffen, & Alais, 2009), in orientation (Apthorp, Wenderoth, & Alais, 2009; Ling & Blake, 2009; Stuit et al., 2009; Stuit, Paffen, van der Smagt, & Verstraten, 2011), and in motion direction (Stuit et al., 2011). We want to clarify, however, what is meant when we use the term "feature-selective suppression." We do not mean that suppression impacts only a limited range of stimuli (e.g., those initially engaged in rivalry). To the contrary, in nearly all published studies using test probes, suppression tends to adversely impact the visibility of a wide range of probe stimuli presented to an eye during suppression (Blake & Fox, 1974; Fox & Check, 1968; Nguyen, Freeman, & Alais, 2003; Wales & Fox, 1970). Indeed, it is this pattern of results that has led to the characterization of binocular rivalry suppression as "non-selective" (for a review of the literature pointing to that characterization, see Blake, 2001). However, the magnitude of that impairment in visibility *does* depend on the specific spatial properties of the stimulus inducing suppression and the stimulus undergoing suppression, and in that sense, we say that suppression is feature selective. In other words, most any new stimulation introduced to an eye whose stimulus is temporarily suppressed will also be adversely impacted (nonselective suppression) but to an extent that depends on the similarity of that new stimulation to the rival targets themselves (feature-selective depth of suppression). Like-wise, to reiterate, interocular suppression generally seems strongest when the dominant stimulus shares features with the suppressed stimulus (e.g., Alais & Melcher, 2007; Alais & Parker, 2006; van de Grind, van Hof, van der Smagt, & Verstraten, 2001). It is interesting to note that feature-selective suppression also exists with dichoptic masking (e.g., Baker & Meese, 2007; Harrad & Hess, 1992; Levi, Harwerth, & Smith, 1979), and there is reason to believe that dichoptic masking and binocular rivalry may be mediated by similar interocular suppression mechanisms (e.g., Baker & Graf, 2009a; van Boxtel, van Ee, & Erkelens, 2007).

Despite similarities between CFS and conventional binocular rivalry, there are a couple of distinct differences between the two. First and foremost, CFS produces considerably longer durations of suppression of the contralateral eye's stimulus than does conventional rivalry stimulation. When they first introduced the CFS technique, Tsuchiya and Koch (2005) famously claimed that "Most observers do not see the image in one eye even though it is present for a long time, sometimes for several minutes (p. 1096)." Such prolonged periods of suppression are never experienced with conventional binocular rivalry stimuli (e.g., Fox & Herrmann, 1967; Levelt, 1965), even when the two eyes' views differ radically in stimulus strength (e.g., Blake, 1977; Fahle, 1982; Fox & Rasche, 1969). What promotes the very robust suppression engendered by the CFS procedure? We agree with Tsuchiya et al. (2006) that the ability of CFS to achieve and maintain dominance for extended periods of time probably has something to do with its relative immunity to neural adaptation. There is, after all, reason to believe that alternations in dominance associated with binocular rivalry arise, in part, from steady weakening of the neural representation of the currently dominant stimulus (e.g., Alais et al., 2010). Perhaps, then, the rapid, repetitive changes in the successively presented, random configurations of a CFS display minimize its tendency to undergo neural adaptation, in a way that cannot happen with static rival targets or even with flickering rival targets whose spatial configurations remain unchanged. Turning to a second notable difference between CFS and binocular rivalry, CFS can elevate test probe thresholds by a log unit or more whereas during conventional binocular rivalry thresholds are elevated no more than 0.5 log unit. By varying the number and timing of flashes comprising CFS, Tsuchiya et al. deduced that the large depth of suppression produced by CFS is attributable to the accumulation of suppressive events associated with the individual, multiple flashes. Those authors also noted that CFS could be construed as a scaled-down version of flash suppression (FS), a technique developed by Wolfe (1984) wherein one eye's rival target is assured dominance by its abrupt presentation very shortly after presentation of the other eye's target.

Returning to a point made earlier in this paper, the 2D amplitude spectrum of the CFS stimulus used in our study reveals that its power is concentrated at lower spatial frequencies. This is evident in the 1D Fourier spectrum obtained by averaging over rotation within the 2D Fourier space (Figure 3). The resulting 1D spectrum conforms to a power law function wherein the amplitude spectrum decreases with increasing spatial frequency (i.e., $1/f^{\alpha}$ where f is spatial frequency and α in the case of multiple samples of this CFS display averages −1.4). Moreover, this power law spectrum is also evidenced in other rival display configurations that produce robust CFS (see Figure S1 for spatial profiles of other CFS stimuli). For that matter, conventional binocular rivalry stimuli whose amplitude spectra resemble the Mondrian CFS profile also strongly dominate rival stimuli with other spectral profiles (Baker & Graf, 2009b). This particularly effective distribution of spatial frequencies is unlikely to be a simple coincidence: It is well known that natural images conform to this spectral profile, too (Field & Brady, 1997; Geisler, 2007), and that the visual system appears to be optimized for encoding this predictable structure in natural scenes (e.g., Simoncelli & Olshausen, 2001). In the case of interocular competition, this optimization reveals itself in the relative strengths of neural responses generated by left- and right-eye stimuli and, by extension, the strength of suppression exerted by those two competing neural representations on one another (Baker & Graf, 2009b). This idea of feature-specific suppression resonates well with the binocular rivalry model by Wilson (2007, later expanded by Shimaoka & Kaneko, 2011) that includes parameters representing neural units that are tuned to different stimulus features of a CFS pattern.

One motive for performing these experiments was to assess whether suppression associated with CFS is feature specific and, by implication, to learn whether the residual effectiveness of a stimulus suppressed by CFS might depend on the low-level features comprising that stimulus. One could argue, of course, that our procedure based on measuring elevations in contrast thresholds reveals very little about the residual effectiveness of a suppressed stimulus. This argument, however, seems overly skeptical, for we know that contrast thresholds are proportional to discriminability (d') which itself is monotonically related to neural responses (e.g., Hawken & Parker, 1990; Tolhurst, Movshon, & Dean, 1983). It does not seem unreasonable to assume, therefore, that contrast thresholds are telling us something important about neural responses associated with visual features of stimuli viewed by the suppressed eye. Now it is true that in some of our test conditions the probe targets were 1D Gabor patches or gratings. However, we purposefully selected that kind of probe target so we could systematically assess spatial frequency selectivity. Gabor patches are widely believed to be optimal stimuli for activating neurons in early stages of visual processing (Olshausen & Field, 1996), and knowing the extent to which CFS selectively impacts visual signals in early visual cortex surely provides some idea of the extent to which later stages of analysis are likely to be impacted given the quality and strength of input to those stages. This, in turn, could provide some clarity to a rapidly growing but increasingly confusing literature on selective visual processing outside of awareness (Adams et al., 2010; Almeida et al., 2008; Costello et al., 2009; Fang & He, 2005; Jiang et al., 2007; E. Yang, Zald, & Blake, 2007, but Gray, Adams, & Garner, 2010; Hesselmann & Malach, 2011; Kang et al., 2011; Kaunitz et al., 2011; Stein et al., 2011; E. Yang et al., 2010). We are not proposing that the engagement of high-level visual processes cannot occur during CFS, but we are concerned that such engagement could be a consequence of the way low-level features were impacted by CFS. At the least, we believe that the present results encourage a reexamination of object-specific suppression by CFS using stimuli whose spatial frequency and orientation content are matched or, at least, explicitly characterized.

Conclusion

The current study systematically investigated the characteristics underlying suppression induced by a popular CFS display. CFS operates by selectively attenuating or abolishing certain low-level signals while leaving others to be potentially encoded during suppression. This feature-selective bias in suppression may be attributed to the spatiotemporal properties of the CFS stimulus and the properties shared with the suppressed stimulus. Findings from the current study suggest the involvement feature-selective mechanisms in neural concomitants of interocular suppression. Furthermore, they suggest that the nature of information that is processed under CFS may be determined by the visual properties of stimuli evoking suppression and of the stimuli being suppressed.

Acknowledgments

This work was supported by NIH EY13358, P30-EY008126, 5T32 EY007135, the National Science Foundation Graduate Research Fellowship (OISE-1107403), and the World Class University Program through the Korea Science and Engineering Foundation funded by the Ministry of Education, Science and Technology (R3110089).

References

Adams WJ, Gray KLH, Garner M, Graf EW. High-level face adaptation without awareness. Psychological Science. 2010; 21:205–210. [PubMed]. [PubMed: 20424046]

Alais D, Cass J, O'Shea RP, Blake R. Visual sensitivity underlying changes in visual consciousness. Current Biology. 2010; 20:1362–1367. [PubMed]. [PubMed: 20598538]

Alais D, Melcher D. Strength and coherence of binocular rivalry depends on shared stimulus complexity. Vision Research. 2007; 47:269–279. [PubMed]. [PubMed: 17049579]

Alais D, Parker A. Independent binocular rivalry processes for motion and form. Neuron. 2006; 52:911–920. [PubMed]. [PubMed: 17145510]

Almeida J, Mahon BZ, Nakayama K, Caramazza A. Unconscious processing dissociates along categorical lines. Proceedings of the National Academy of Sciences of the United States of America. 2008; 105:15214–15218. [PubMed]. [PubMed: 18809923]

Apthorp D, Wenderoth P, Alais D. Motion streaks in fast motion rivalry cause orientation-selective suppression. Journal of Vision. 2009; 9(5):10, 1–14. http://www.journalofvision.org/content/9/5/10, doi:10.1167/9.5.10. [PubMed] [Article]. [PubMed: 19757888]

Bahrami B, Lavie N, Rees G. Attentional load modulates responses of human primary visual cortex to invisible stimuli. Current Biology. 2007; 17:509–513. [PubMed]. [PubMed: 17346967]

Baker DH, Graf EW. On the relation between dichoptic masking and binocular rivalry. Vision Research. 2009a; 49:451–459. [PubMed]. [PubMed: 19124036]

Baker DH, Graf EW. Natural images dominate in binocular rivalry. Proceedings of the National Academy of Sciences of the United States of America. 2009b; 106:5436–5441. [PubMed]. [PubMed: 19289828]

Baker DH, Meese TS. Binocular contrast interactions: Dichoptic masking is not a single process. Vision Research. 2007; 47:3096–3107. [PubMed]. [PubMed: 17904610]

Blake R. Threshold conditions for binocular rivalry. Journal of Experimental Psychology. 1977; 3:251–257. [PubMed]. [PubMed: 864397]

Blake R. Primer on binocular rivalry, including controversial issues. Brain & Mind. 2001; 2:5–38.

Blake R, Fox R. Binocular rivalry suppression: Insensitive to spatial frequency and orientation change. Vision Research. 1974; 14:687–692. [PubMed]. [PubMed: 4418766]

Blake R, Tadin D, Sobel KV, Raissian TA, Chong SC. Strength of early visual adaptation depends on visual awareness. Proceedings of the National Academy of Sciences of the United States of America. 2006; 103:4783–4788. [PubMed]. [PubMed: 16537384]

Blake R, Yu K, Lokey M, Norman H. Binocular rivalry and motion perception. Journal of Cognitive Neuroscience. 1998; 10:46–60. [PubMed]. [PubMed: 9526082]

Brainard DH. The psychophysics toolbox. Spatial Vision. 1997; 10:433–436. [PubMed: 9176952]

Campbell FW, Robson JG. Application of Fourier analysis to the visibility of gratings. The Journal of Physiology. 1968; 197:551–566. [PubMed]. [PubMed: 5666169]

Carmel D, Arcaro M, Kastner S, Hasson U. How to create and use binocular rivalry. Journal of Visualized Experiments. 2010; 45:1–10. [PubMed].

Costello P, Jiang Y, Baartman B, McGlennen K, He S. Semantic and subword priming during binocular suppression. Consciousness and Cognition. 2009; 18:375–382. [PubMed]. [PubMed: 19286396]

Fahle M. Binocular rivalry: Suppression depends on orientation and spatial frequency. Vision Research. 1982; 22:787–800. [PubMed]. [PubMed: 7123863]

Fang F, He S. Cortical responses to invisible objects in the human dorsal and ventral pathways. Nature Neuroscience. 2005; 8:1380–1385. [PubMed].

Field DJ, Brady N. Visual sensitivity, blur and the sources of variability in the amplitude spectra of natural scenes. Vision Research. 1997; 37:3367–3383. [PubMed]. [PubMed: 9425550]

Fox R, Check R. Detection of motion during binocular rivalry suppression. Journal of Experimental Psychology. 1968; 78:388–395. [PubMed]. [PubMed: 5705853]

Fox R, Herrmann J. Stochastic properties of binocular rivalry alternations. Perception & Psychophysics. 1967; 2:432–436. [PubMed].

Fox R, Rasche F. Binocular rivalry and reciprocal inhibition. Perception & Psychophysics. 1969; 5:215–217.

Geisler WS. Visual perception and the statistical properties of natural scenes. Annual Review in Psychology. 2007; 59:167–192. [PubMed].

Gray K, Adams W, Garner M. Preferential processing of fear faces: Emotional content vs. low-level visual properties [Abstract]. Journal of Vision. 2010; 10(7):610, 610a. http://www.journalofvision.org/content/10/7/610, doi:10.1167/10.7.610.

Hansen BC, Essock EA. Anisotropic local contrast normalization: The role of stimulus orientation and spatial frequency bandwidths in the oblique and horizontal effect perceptual anisotropies. Vision Research. 2006; 46:4398–4415. [PubMed]. [PubMed: 17027896]

Harrad RA, Hess RF. Binocular integration of contrast information in amblyopia. Vision Research. 1992; 32:2135–2150. [PubMed]. [PubMed: 1304091]

Hawken, MJ.; Parker, AJ. Detection and discrimination mechanisms in the striate cortex of the Old-World monkey. In: Blakemore, C., editor. Vision: Coding and efficiency. Cambridge University Press; New York: 1990. p. 103-116.

Hesselmann G, Malach R. The link between fMRI-BOLD activation and perceptual awareness is “stream-invariant” in the human visual system. Cerebral Cortex. 2011; 21:2829–2837. [PubMed]. [PubMed: 21515713]

Hollins M, Hudnell K. Adaptation of the binocular rivalry mechanism. Investigative Ophthalmology & Visual Science. 1980; 19:1117. [PubMed]. [PubMed: 7410003]

Hong SW, Blake R. Interocular suppression differentially affects achromatic and chromatic mechanisms. Attention, Perception & Psychophysics. 2009; 71:403–420. [PubMed].

Jiang Y, Costello P, He S. Processing of invisible stimuli: Advantage of upright faces and recognizable words in overcoming interocular suppression. Psychological Science. 2007; 18:349–355. [PubMed]. [PubMed: 17470261]

Jiang Y, He S. Cortical responses to invisible faces: Dissociating subsystems for facial-information processing. Current Biology. 2006; 16:2023–2029. [PubMed]. [PubMed: 17055981]

Kanai R, Tsuchiya N, Verstraten FAJ. The scope and limits of top-down attention in unconscious visual processing. Current Biology. 2006; 16:2332–2336. [PubMed]. [PubMed: 17141615]

Kang M-S, Blake R, Woodman GF. Semantic analysis does not occur in the absence of awareness induced by interocular suppression. Journal of Neuroscience. 2011; 31:13535–13545. [PubMed]. [PubMed: 21940445]

Kaunitz LN, Kamienkowski JE, Olivetti E, Murphy B, Avesani P, Melcher DP. Intercepting the first pass: Rapid categorization is suppressed for unseen stimuli. Frontiers in Psychology. 2011; 2:1–10. [PubMed]. [PubMed: 21713130]

Levelt, WJM. Soesterberg. Institute for Perception RVO-TNO; The Netherlands: 1965. On binocular rivalry.

Levi DM, Harwerth RS, Smith EL 3rd. Humans deprived of normal binocular vision have binocular interactions tuned to size and orientation. Science. 1979; 206:852–854. [PubMed]. [PubMed: 493988]

Levitt H. Transformed up–down methods in psychoacoustics. The Journal of the Acoustical Society of America. 1971; 49:467. [PubMed]. [PubMed: 5541744]

Lin ZC, He S. Seeing the invisible: The scope and limits of unconscious processing in binocular rivalry. Progress in Neurobiology. 2009; 87:195–211. [PubMed]. [PubMed: 18824061]

Ling S, Blake R. Suppression during binocular rivalry broadens orientation tuning. Psychological Science. 2009; 20:1348–1355. [PubMed]. [PubMed: 19788529]

Lundqvist, D.; Litton, J. Department of Clinical Neuroscience, Psychology section. Karolinska Institutet; Solna, Sweden: 1998. The Averaged Karolinska Directed Emotional Faces—AKDEF.

Maruya K, Watanabe H, Watanabe M. Adaptation to invisible motion results in low-level but not high-level aftereffects. Journal of Vision. 2008; 8(11):7, 1–11. http://www.journalofvision.org/content/8/11/7, doi:10.1167/8.11.7. [PubMed] [Article]. [PubMed: 18831601]

Nguyen VA, Freeman AW, Alais D. Increasing depth of binocular rivalry suppression along two visual pathways. Vision Research. 2003; 43:2003–2008. [PubMed]. [PubMed: 12842153]

Nguyen VA, Freeman AW, Wenderoth P. The depth and selectivity of suppression in binocular rivalry. Perception & Psychophysics. 2001; 63:348–360. [PubMed]. [PubMed: 11281109]

Olshausen BA, Field DJ. Emergence of simple-cell receptive field properties by learning a sparse code for natural images. Nature. 1996; 381:607–609. [PubMed]. [PubMed: 8637596]

O'Shea RP, Sims AJ, Govan DG. The effect of spatial frequency and field size on the spread of exclusive visibility in binocular rivalry. Vision Research. 1997; 37:175–183. [PubMed]. [PubMed: 9068818]

Pelli DG. The VideoToolbox software for visual psychophysics: Transforming numbers into movies. Spatial Vision. 1997; 10:437–442. [PubMed]. [PubMed: 9176953]

Shimaoka D, Kaneko H. Dynamical systems modeling of continuous flash suppression. Vision Research. 2011; 51:521–528. [PubMed]. [PubMed: 21296102]

Shin K, Stolte M, Chong SC. The effect of spatial attention on invisible stimuli. Attention, Perception & Psychophysics. 2009; 71:1507–1513. [PubMed].

Simoncelli EP, Olshausen BA. Natural image statistics and neural representation. Annual Review of Neuroscience. 2001; 24:1193–1216. [PubMed].

Stein T, Hebart MN, Sterzer P. Breaking continuous flash suppression: A new measure of unconscious processing during interocular suppression? Frontiers in Human Neuroscience. 2011; 5:1–17. [PubMed]. [PubMed: 21283556]

Stein T, Sterzer P. High-level face shape adaptation depends on visual awareness: Evidence from continuous flash suppression. Journal of Vision. 2011; 11(8):5, 1–14. http://www.journalofvision.org/content/11/8/5, doi:10.1167/11.8.5. [PubMed] [Article]. [PubMed: 21742962]

Sterzer P, Jalkanen L, Rees G. Electromagnetic responses to invisible face stimuli during binocular suppression. Neuroimage. 2009; 46:803–808. [PubMed]. [PubMed: 19285140]

Stuit SM, Cass J, Paffen CLE, Alais D. Orientation-tuned suppression in binocular rivalry reveals general and specific components of rivalry suppression. Journal of Vision. 2009; 9(11):17, 1–15. http://www.journalofvision.org/content/9/11/17, doi:10.1167/9.11.17. [PubMed] [Article].

Stuit SM, Paffen CL, van der Smagt MJ, Verstraten FA. Suppressed images selectively affect the dominant percept during binocular rivalry. Journal of Vision. 2011; 11(10):7, 1–11. http://www.journalofvision.org/content/11/10/7, doi:10.1167/11.10.7. [PubMed] [Article]. [PubMed: 21920853]

Tolhurst DJ, Movshon JA, Dean AF. The statistical reliability of signals in single neurons in cat and monkey visual cortex. Vision Research. 1983; 23:775–785. [PubMed]. [PubMed: 6623937]

Tsuchiya N, Koch C. Continuous flash suppression reduces negative afterimages. Nature Neuroscience. 2005; 8:1096–1101. [PubMed].

Tsuchiya N, Koch C, Gilroy LA, Blake R. Depth of interocular suppression associated with continuous flash suppression, flash suppression, and binocular rivalry. Journal of Vision. 2006; 6(10):6, 1068–1078. http://www.journalofvision.org/content/6/10/6, doi:10.1167/6.10.6. [PubMed] [Article].

Tyler CW. Colour bit-stealing to enhance the luminance resolution of digital displays on a single pixel basis. Spatial Vision. 1997; 10:369–377. [PubMed]. [PubMed: 9176946]

van Boxtel JJA, van Ee R, Erkelens CJ. Dichoptic masking and binocular rivalry share common perceptual dynamics. Journal of Vision. 2007; 7(14):3, 1–11. http://www.journalofvision.org/content/7/14/3, doi:10.1167/7.14.3. [PubMed] [Article]. [PubMed: 18217798]

van de Grind WA, van Hof P, van der Smagt MJ, Verstraten FA. Slow and fast visual motion channels have independent binocular-rivalry stages. Proceedings of the Royal Society of London B: Biological Sciences. 2001; 268:437–443. [PubMed].

Wales R, Fox R. Increment detection thresholds during binocular rivalry suppression. Perception & Psychophysics. 1970; 17:571–577.

Watson AB, Pelli DG. Quest—A Bayesian Adaptive Psychometric method. Perception & Psychophysics. 1983; 33:113–120. [PubMed]. [PubMed: 6844102]

Wilson HR. Minimal physiological conditions for binocular rivalry and rivalry memory. Vision Research. 2007; 47:2741–2750. [PubMed]. [PubMed: 17764714]

Wolfe JM. Reversing ocular dominance and suppression in a single flash. Vision Research. 1984; 24:471–478. [PubMed]. [PubMed: 6740966]

Yang E, Hong SW, Blake R. Adaptation aftereffects to facial expressions suppressed from visual awareness. Journal of Vision. 2010; 10(12):24, 1–13. http://www.journalofvision.org/content/10/12/24, doi:10.1167/10.12.24. [PubMed] [Article]. [PubMed: 21047756]

Yang E, Zald DH, Blake R. Fearful expressions gain preferential access to awareness during continuous flash suppression. Emotion. 2007; 7:882–886. [PubMed]. [PubMed: 18039058]

Yang Y, Rose D, Blake R. On the variety of percepts associated with dichoptic viewing of dissimilar monocular stimuli. Perception. 1992; 21:47–62. [PubMed]. [PubMed: 1528703]

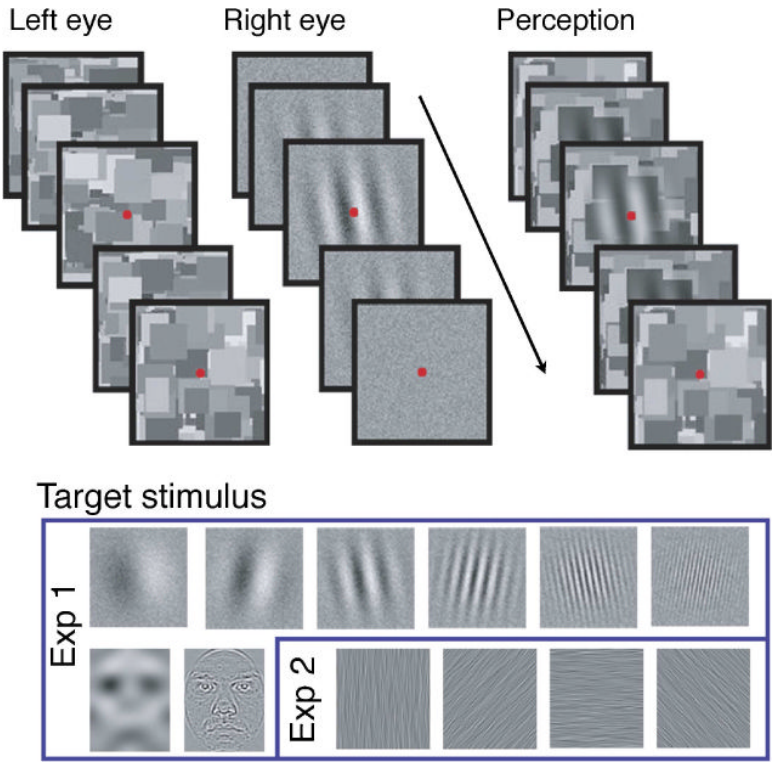

Figure 1.
Illustration of a trial sequence including CFS in Experiment 1 (top) and sample images of the target stimuli in Experiments 1 and 2 (bottom). Exp = Experiment.

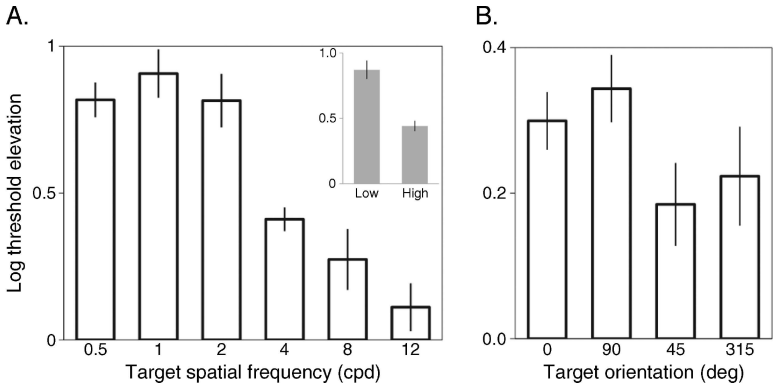

Figure 2.

Results of (left) Experiments 1 and (right) 2. The mean elevations in contrast threshold (log scaled) as a function of the spatial frequency or orientation of the target stimulus (Gabor patch or orientation band-pass filtered noise) that was suppressed with CFS are plotted. The inset in the left graph pertains to threshold elevations for detecting low or high spatial frequency band-pass filtered face images. Error bars denote the standard error of the mean *(SEM)*.

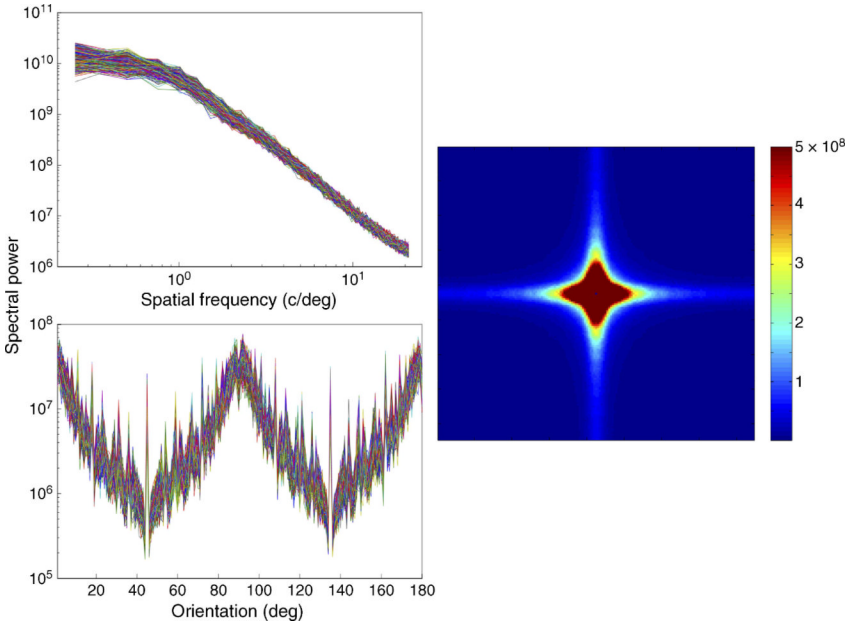

Figure 3.

(Left) One-dimensional and (right) two-dimensional Fourier power spectra of 1000 randomly generated Mondrian images (4° × 4°, 50% RMS contrast). Colors in the left figures denote the (top) spatial frequency and (bottom) orientation power spectra of a given Mondrian image. Colors in the right figure depict the mean spectral power at different spatial frequencies and orientations, which are denoted by the distance from the origin and polar angle, respectively.

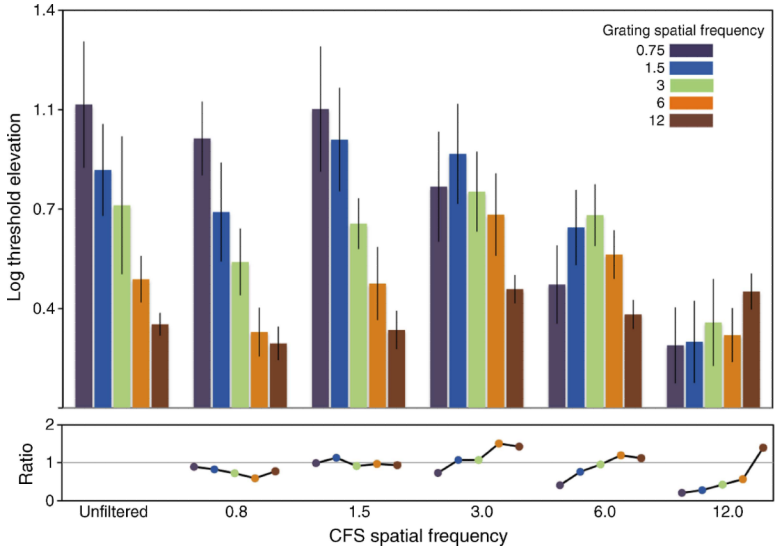

Figure 4.

Results of Experiment 3. The bar graph depicts elevations in contrast threshold for detecting a grating with a given spatial frequency (color) as a function of the spatial frequency range in the CFS display (set of bars). The bottom line graph is a different depiction of the top graph. The ratio of log threshold elevation for detecting a grating under a given band-pass filtered CFS display and detecting that same spatial frequency grating under the unfiltered CFS display (leftmost set of bars) is plotted. Values below 1 indicate that the filtered CFS condition produced weaker elevations in thresholds relative to the unfiltered CFS condition. Abscissa denotes the center frequency of the band-pass filter. Error bars denote *SEM*.

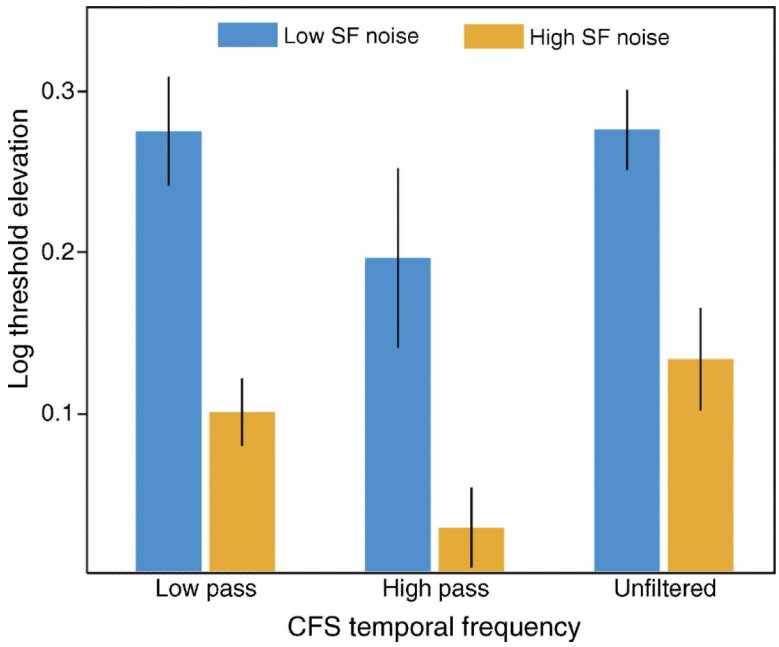

Figure 5.
Results of Experiment 4. The mean elevations in threshold for detecting a low (blue) or high (orange) spatial frequency (SF) band-pass filtered probe stimulus that was suppressed with either a temporal low-pass, high-pass, or unfiltered CFS display are plotted. Error bars represent *SEM*.